Wave Motion 48 (2011) 176–183

Contents lists available at ScienceDirect

Wave Motion

journal homepage: www.elsevier.com/locate/wavemoti

Effect of viscosity on dispersion of capillary–gravity waves

F. Behroozi *, J. Smith [1], W. Even [2]

Department of Physics, University of Northern Iowa, Cedar Falls, IA, United States

ARTICLE INFO

Article history:
Received 13 March 2010
Received in revised form 26 September 2010
Accepted 29 September 2010
Available online 16 October 2010

Keywords:
Dispersion relation
Capillary waves
Wave attenuation
Viscosity

ABSTRACT

The effect of viscosity on dispersion of capillary–gravity waves becomes significant when the attenuation coefficient is greater than about 2.5% of the wave number. For low viscosity fluids such as water this condition is met at frequencies greater than about 5 kHz in which case direct measurement of wavelength is difficult. For higher viscosity fluids the effect appears at much lower frequencies but direct measurement of wavelength becomes difficult since viscosity causes severe attenuation of surface waves. We have overcome the measurement difficulties by using a new miniature laser interferometer, which directly measures the wavelength of standing capillary waves with the requisite precision to yield reliable dispersion data for viscous fluids. Here we review the effect of viscosity on the dispersion relation and present new experimental data on dispersion of capillary waves in several water-glycerol mixtures. Our data provides direct experimental verification of the theoretical analysis.

1. Introduction

It is well known that the dispersion of capillary waves is affected by fluid viscosity [1,2]. In practice, the effect of viscosity becomes significant when the attenuation coefficient α is greater than about 2.5% of the wave number k_0. For low viscosity fluids such as water this condition is met when the frequency exceeds about 5 kHz. However, at 5 kHz the wavelength is about 0.25 mm, making a direct measurement of the wavelength rather unreliable. In contrast, for a 50% mixture of glycerin in water, the attenuation coefficient α approaches 5% of the wave number k_0 at a frequency of 250 Hz. Therefore, to study the effect of viscosity on dispersion of capillary waves the more practical option is to measure the effect in fluids of higher viscosity.

The dispersion of capillary waves has been studied mostly by photon correlation spectroscopy [3–7]. The experimental technique analyzes line broadening of scattered light from thermally excited capillary waves to infer dispersion and attenuation data [8–12]. However, with thermally excited capillary waves, one is naturally limited to waves in the micron length regime, typically from about 500 μm down to about 5 μm. At these wavelengths, the frequency is in the range of 1.8 MHz to 10 GHz in which case waves are severely attenuated even when the fluid has a very low viscosity. Furthermore, for thermal capillary waves with submicron wavelength where X-rays are used as probes, a further complication is a significant reduction of surface energy of liquid interfaces [13]. Nevertheless, interest in the technique remains high principally because light scattering and correlation spectroscopy are well-developed areas of optics [5] and partly because the technique is well adapted for use with X-rays [14]. It should be mentioned, however, that some researchers have used surface light scattering to study the effect of viscosity on single frequency capillary waves [15–17] with some success.

We have recently developed a new and improved method for measuring the wavelength and amplitude of single frequency capillary waves by using a miniature laser interferometer. Our measurement method which is partly based on earlier work by others [18–20], is described in more detail elsewhere [21–23]. It allows us to generate single-frequency standing waves in the millimeter wavelength regime and to measure the wavelength and amplitude of the waves noninvasively. The resulting dispersion

* Corresponding author.
E-mail address: behroozi@uni.edu (F. Behroozi).
[1] Current Address: Sandia National Laboratories, Box 5800, Albuquerque, NM 87185, United States.
[2] Current Address: Department of Physics, Louisiana State University, Baton Rouge, LA 70803, United States.

0165-2125/$ – see front matter © 2010 Elsevier B.V. All rights reserved.
doi:10.1016/j.wavemoti.2010.09.002

data contains the requisite precision to show unambiguously the effect of viscosity on propagation of capillary waves at frequencies below 2 kHz, and provides very reliable experimental data for comparison with theory.

2. Theoretical background

The full dispersion relation for capillary–gravity waves on simple fluids appears in the classic text by H. Lamb [1], which in modern notation may be written [2,3], as a complex equation:

$$(i\omega + 2\eta k^2/\rho)^2 + g\,k + \sigma k^3/\rho = (4\eta^2 k^3/\rho^2)\,(k^2 + i\omega\rho/\eta)^{1/2} \tag{1}$$

The symbols denote the usual quantities; ω is the angular frequency, η denotes the viscosity, k is the complex wave vector, ρ stands for density, g is the acceleration of gravity, and σ represents the surface tension. Following common practice, let

$$k = k_0 - i\alpha,$$

where $k_0 = 2\pi/\lambda$ is the wave number, and α stands for the attenuation coefficient.

In the absence of viscosity, Eq. (1) reduces to the familiar and simple dispersion relation,

$$\omega^2 = g\,k_0 + \sigma k_0^3/\rho \tag{2}$$

Furthermore, to compare the experimental dispersion data with the predictions of Eq. (1), we apply a few sensible approximations that are valid in the capillary limit, and then proceed to separate the complex equation into two, one involving the real terms, and the other involving the leading imaginary terms.

In the capillary wave regime since $\omega\rho/k^2\eta >> 1$, we use the following approximation in Eq. (1),

$$(k^2 + i\omega\rho/\eta)^{1/2} \approx (1+i)(\omega\rho/2\eta)^{1/2}$$

to get,

$$\omega^2 = gk + (4i\omega\eta/\rho)k^2 + [\sigma/\rho - (1+i)(\omega^{1/2}2^{3/2}\eta^{3/2}/\rho^{3/2})]k^3 + (4\eta^2/\rho^2)k^4 \tag{3}$$

On substituting the following approximate expressions for k, k^2, k^3, and k^4 in Eq. (3)

$$k = k_0 - i\alpha$$
$$k^2 \approx \left(k_0^2 - 2ik_0\alpha\right)$$
$$k^3 \approx \left(k_0^3 - 3ik_0^2\alpha\right)$$
$$k^4 \approx \left(k_0^4 - 4ik_0^3\alpha\right)$$

we obtain,

$$\omega^2 = +g(k_0 - i\alpha) + (4i\omega\eta/\rho)\left(k_0^2 - 2ik_0\alpha\right) + [\sigma/\rho - (1+i)(\omega^{1/2}2^{3/2}\eta^{3/2}/\rho^{3/2})]\left(k_0^3 - 3ik_0^2\alpha\right) + (4\eta^2/\rho^2)\left(k_0^4 - 4ik_0^3\alpha\right) \tag{4}$$

Eq. (4) can be separated into two equations, one real, and one imaginary. Keeping just the two leading terms in the imaginary equation, we get

$$4\omega k_0^2\eta/\rho \approx +3k_0^2\alpha\sigma/\rho \tag{5}$$

Eq. (5) immediately yields the approximate expression for the attenuation coefficient in the capillary wave limit,

$$\alpha \approx 4\omega\eta/3\sigma \tag{6}$$

Substituting for α in Eq. (4), and keeping only the leading real terms results in the approximate dispersion relation for the capillary waves,

$$\omega^2 = gk_0 + [\sigma/\rho - (8\eta^3\omega/\rho^3)^{1/2} + 4(k_0\eta^2/\rho^2)]k_0^3 \tag{7}$$

In light of Eqs. (2),(7), states that the effect of viscosity on the dispersion relation may be regarded as a correction to the surface tension. Note that in the absence of viscosity, Eq. (7) reverts back to the simple form of Eq. (2). In this case a plot of ω^2/k_0 vs. k_0^2 gives a straight line with a slope of σ/ρ. However, when viscosity cannot be ignored, the presence of the two competing η-dependent terms

in Eq. (7) influences the slope of the ω^2/k_0 vs. k_0^2 graph. It is worth noting that for low viscosity fluids such as water, the two terms are small and essentially cancel one another for frequencies below about 5 kHz with little effect on the plot of ω^2/k_0 vs. k_0^2. For liquids of higher viscosity, the $\eta^{3/2}$-term dominates as the frequency and thus k_0^2 is increased, causing the ω^2/k_0 vs. k_0^2 graph to turn downward.

3. Experimental details

The experimental technique for generation and detection of capillary waves has been described in some detail elsewhere [21–23]. Here we present a brief summary and provide some more details on the special features used in the current experiments.

As shown in Fig. 1, capillary waves are generated electronically by placing a metallic blade a few tenths of a millimeter above the fluid surface. A dc-biased sinusoidal voltage of a few hundred volts at the selected frequency is applied between the blade and the fluid. For polar fluids such as water or water based binary mixtures, the alternating electric field under the blade generates two capillary wave trains that recede from the blade on each side. Typically the amplitude of these waves is less than 1 μm. Since the wavelength of the capillary waves is a fraction of the depth of the trough, the deep fluid formalism applies.

Fig. 1 is a schematic of one wave generating blade and a fiber probe above the capillary wave. The fiber-optic probe is mounted on an electronic micrometer, which records the probe position on the surface with an accuracy of about ± 1 μm. The distance from the tip of the probe to the equilibrium surface is d_o, and the roundtrip distance between the tip of the probe and the fluid surface, i.e., the path difference between the two reflected beams, is Δ. A typical wavelength is about one mm, and typical wave amplitude is less than one micrometer. In this schematic the wave amplitude has been vastly exaggerated for clarity.

The schematic of the electro-optical system is shown in Fig. 2. A small fraction of the laser light is split by the cube splitter for use as a reference signal at the detector to compensate for any laser output fluctuations. The main beam passes through a birefringent cube and is split into two equal beams for use in the two fiber optic probes. The Gould multiplexer with one input and two outputs is essential in routing the interference signal to the detector and blocking the return path to the laser. The multiplexer directs the returning interference signal to the other output and thus isolates the outputs from the input. The Faraday rotator further isolates and protects the laser cavity from "seeing" any reflected signal by changing the polarization direction of any reflected light that may find its way back to the laser.

The interference signal is detected, amplified, and digitized for later analysis. In Fig. 3 we give a typical interference signal. The raw interference signal for a half period is shown at the top of the frame. The solid curve is the mathematical fit, which replicates the trace faithfully. The dashed curve gives the vertical displacement of the surface wave under the probe as a function of time. The right scale is for the interference signal and the left scale is for the wave amplitude.

Since there is a one to one correspondence between the surface wave and the resulting interference pattern, the profile of the surface wave can be recovered by an analysis of the interference pattern. Indeed, the number of fringes in the interference pattern is directly proportional to the amplitude of the surface wave [24]. For the pattern shown in Fig. 3, the number of fringes is 6.78 and the amplitude of the wave is 1.07 μm.

A standing wave is generated when two waves of the same frequency and amplitude move in the same space but in opposite directions. This is the case when two blades are used to generate waves of the same amplitude and frequency. Since each blade sends a wave train toward the other, a standing capillary wave is established on the surface between the two blades. If the distance between the two blades is chosen to be a half odd-integer wavelength, i.e. $(2n+1)\lambda/2$, the two wave trains interfere destructively on the outer sides of the blades. This judicious choice of the blades' separation produces a region of standing waves between the blades while the fluid surface outside the blades remains calm thus effectively eliminating any wave reflections from the far boundaries of the trough. The second fiber probe shown in Fig. 2 is used to ensure this condition obtains. Typically a distance of about ten wavelengths separates the blades. It should be mentioned that at the higher frequencies the attenuation is strong enough that the reflection from the boundaries is no longer a problem.

When a standing wave is established on the fluid surface, accurate measurement of the distance between several nodes determines the wavelength very accurately. This is accomplished by moving the fiber-optic probe over the fluid surface between

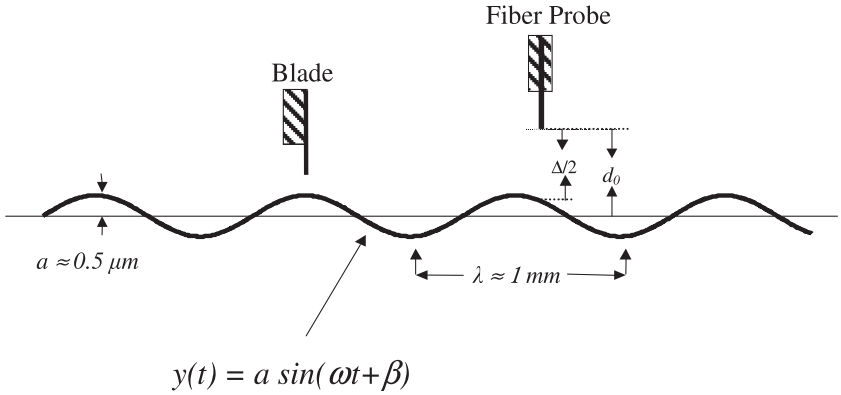

Fig. 1. Schematic of a fiber optic probe and a wave-generating blade above the fluid surface.

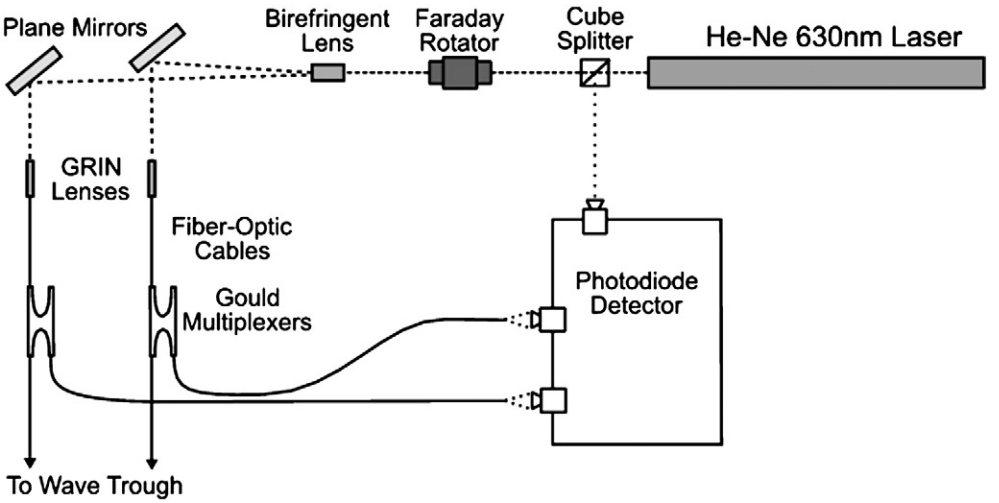

Fig. 2. Schematic of the optical and electronic detection system.

the blades. As the probe moves over nodes and antinodes, the interference fringe count peaks at an antinode and diminishes to zero over a node. Thus it is possible to count the number of nodes as the probe scans the surface. Since a digital micrometer monitors the probe's position, we can measure the wavelength of the standing capillary waves to within one micrometer.

At higher frequencies when attenuation is strong, it is impractical to establish standing waves. In this case, only one blade is used to generate a wave train. A probe is used to scan the fluid surface starting from a point as close to the exciting blade as possible and moving away. The interference pattern on the digital scope shifts through a complete period as the probe on the surface travels through a wavelength. In this way the probe may be moved through several wavelengths as the interference pattern on the scope shifts through the same number of time periods. The micrometer reading gives an accurate measure of the wavelength.

4. Results and discussion

We chose the well-studied water-glycerin binary mixture to explore the effect of viscosity on dispersion of capillary waves. Several glycerin–water mixtures were prepared with glycerin concentrations ranging from 5% to 90%. Reagent quality glycerin (purity, 99.99%) and highly purified and deionized water (resistivity, 18 MΩ m) were used to make these mixtures.

To study the effect for a wide range of viscosities and frequencies we obtained dispersion data on water–glycerin binary mixtures with glycerin concentrations ranging from 5% to 90% and at frequencies from 10 Hz up to about 2 kHz. For mixtures with glycerin concentration over 75% the wave attenuation was too severe to obtain reliable data for wavelengths less than 2 mm.

A Teflon trough (6 cm by 46 cm, with depth of 1 cm) was used to contain the liquid under study. Thermoelectric cells underneath the trough were used to regulate the temperature. To minimize air currents and mechanical disturbances, the experimental system was housed in an enclosure and placed on an isolation table.

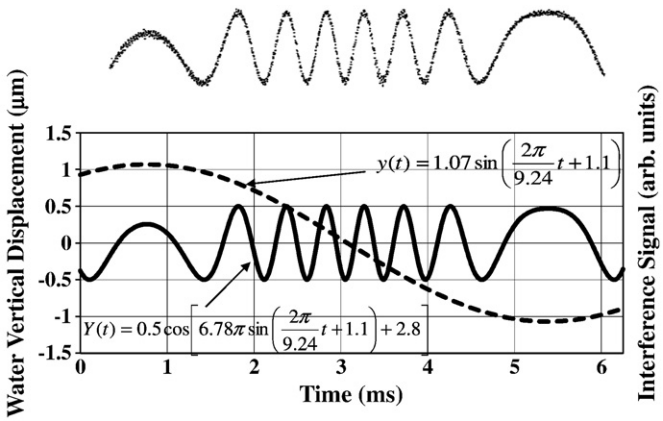

Fig. 3. The interference signal for one half-wavelength. The raw interference signal for the half period is shown at the top of the frame. The solid curve is the mathematical fit, which replicates the trace faithfully. The dashed curve gives the vertical displacement of the surface wave under the probe as a function of time.

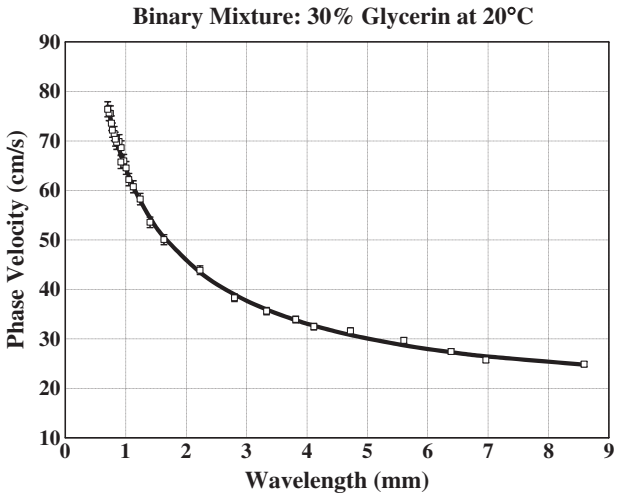

Fig. 4. Phase velocity of capillary waves as a function of wavelength at 20 °C for a glycerin–water binary mixture with 30% glycerin concentration. The solid line is a fit using Eq. (9) in the text.

The dispersion data on each of the mixtures was obtained by measuring the wavelength of the capillary waves at a wide range of frequencies starting from about 10 Hz up to the highest frequency for which reliable measurement of the wavelength was possible. For a binary mixture the highest frequency for which wavelength measurement is reliable depends on the glycerin concentration. This is because the viscosity of the mixture increases with glycerin concentration, which in turn causes severe wave attenuation as a function of distance from the source, particularly at higher frequencies. In other words, as the glycerin concentration increases, the amplitude of the wave decreases rapidly over a short distance from the generating blade making reliable wavelength measurements difficult. For example at a glycerin concentration of 70%, we were able to measure the wavelength reliably only up to a frequency of 167 Hz. On the other hand at 30% glycerin concentration wavelength measurement were performed up to 1093 Hz.

The effect of viscosity on the dispersion of capillary waves becomes apparent at glycerin concentrations above 50%. At lower concentrations, the effect becomes noticeable only at very high frequencies, typically above 5 kHz, in which case it is difficult to obtain reliable wavelength data due to sever amplitude attenuation which results in very small extinction distance.

As an example and for later comparison we will first discuss the dispersion data for a binary mixture with 30% glycerin. Fig. 4 gives the experimental phase velocity $v_\varphi = f\lambda$ as a function of wavelength at 20 °C. The solid line through the data is the fit expressed in Eq. (8) which is derived from Eq. (2),

$$v_\varphi = \omega / k_0 = (g/k_0 + \sigma k_0/\rho)^{1/2} \tag{8}$$

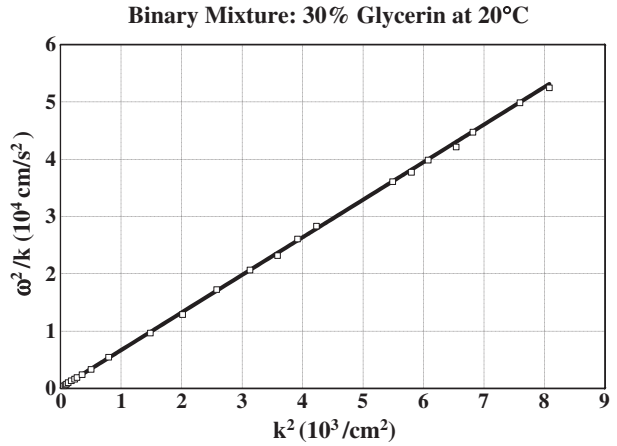

Fig. 5. Dispersion data for capillary waves plotted as ω^2/k_0 vs. k_0^2 for the binary mixture with 30% glycerin at 20 °C. The solid line is a fit using Eq. (10) in the text. The slope gives the value of surface tension over density (σ/ρ) for this mixture.

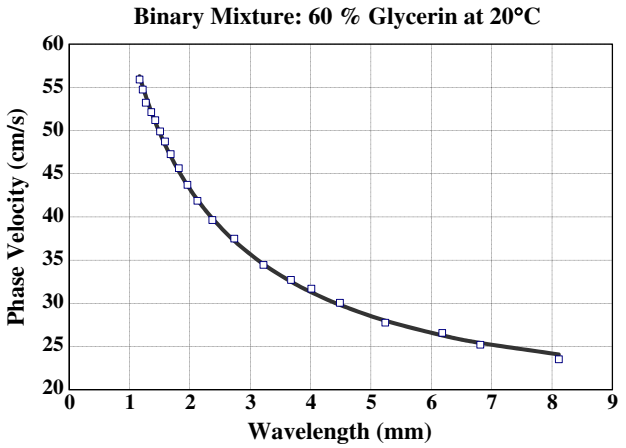

Fig. 6. Phase velocity of capillary waves as a function of wavelength at 20 °C for a glycerin–water binary mixture with 60% glycerin concentration. The solid line is a fit using Eq. (9) in the text.

In this expression, viscosity is neglected and the only adjustable parameter is σ/ρ. For this data set the best fit is obtained when σ/ρ is set to 65.75 dynes cm^2/g. If instead of Eq. (2), we use Eq. (7), the expression for phase velocity is given by

$$v_\varphi = \{g/k_0 + k_0[\sigma/\rho - (8\eta^3\omega/\rho^3)^{1/2} + 4k_0\eta^2/\rho^2]\}^{1/2} \tag{9}$$

When Eq. (9) is used to fit the 30%-glycerin data the result is indistinguishable from that of the solid line in Fig. 4. This is because each of the two terms on the right side of Eq. (9) involving viscosity is less than one percent of the σ/ρ term even at a frequency of 1 kHz. Indeed at 30% concentration, the kinematic viscosity $\eta/\rho = 0.02$ cm^2/s, so at a frequency of one kHz the fist term is about 0.6 in cgs units which is less than one percent of the σ/ρ term. Furthermore the second term involving viscosity is of the same order of magnitude but since it has an opposite sign, the two terms tend to cancel each other.

The effect of viscosity is revealed more effectively when the dispersion data is plotted as ω^2/k_0 vs. k_0^2. This is because when the dispersion relation as given in Eq. (7) is recast in the form

$$\omega^2/k_0 = g + [\sigma/\rho - (8\eta^3\omega/\rho^3)^{1/2} + 4k_0\eta^2/\rho^2]k_0^2 \tag{10}$$

the resulting graph is linear when the effect of viscosity is negligible. However at higher frequencies and viscosity the slope will be affected.

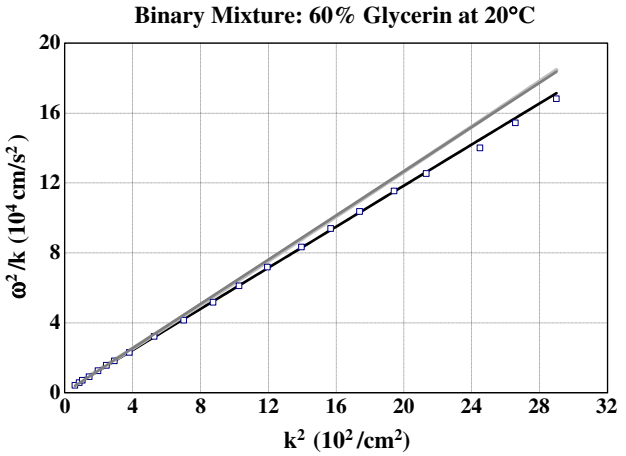

Fig. 7. Dispersion data for capillary waves plotted as ω^2/k_0 vs. k_0^2 for the binary mixture with 60% glycerin at 20 **°C**. The solid line is a fit using Eq. (10) in the text. The gray line is a fit using Eq. (11), which does not take the effect of viscosity into account.

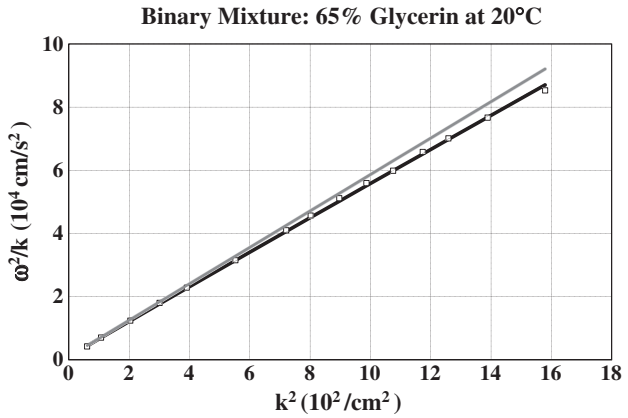

Fig. 8. Dispersion data for capillary waves plotted as ω^2/k_0 vs. k_0^2 for the binary mixture with 65% glycerin at 20 °C. The solid line is a fit using Eq. (10) in the text. The gray line is a fit using Eq. (11), which does not take the effect of viscosity into account.

In fact we expect that at higher viscosity, the $(8\eta^3\omega/\rho^3)^{1/2}$ term will overtake the $(4k_0\eta^2/\rho^2)$ term at higher frequencies and cause a downward curvature in the plot of ω^2/k_0 vs. k_0^2. In Fig. 5, the graph of (ω^2/k_0) vs. k_0^2 for the 30% data shows no such curvature. Indeed the solid line is the fit using Eq. (10) with the appropriate parameters, namely $\sigma/\rho = 65.75$ dyne cm^2/g, and $\eta/\rho = 0.02$ cm^2/s. The fit is just as good if we set $\eta = 0$ in Eq. (10) and use the simple version shown in Eq. (11),

$$\omega^2 / k_0 = g + (\sigma/\rho)k_0^2 \tag{11}$$

In contrast the data for 60% glycerin concentration (Figs. 6, and 7) clearly show the effect of viscosity on dispersion. In Fig. 6 the solid line is the fit using Eq. (9) with $\sigma/\rho = 58.5$ dyne cm^2/g, and $\eta/\rho = 0.044$ cm^2/s. The effect of viscosity is revealed more dramatically in Fig. 7. The solid black line through the data points is the fit based on Eq. (10), with the same parameters given above. The gray line is the fit using Eq. (11), which neglects viscosity. Clearly the effect of viscosity is to cause the slope of the graph to moderate as the frequency is increased.

The effect becomes pronounced at much lower frequencies as the viscosity is increased. Figs. 8, and 9 give the data for glycerin concentrations of 65% and 70%. Note that the departure of ω^2/k_0 vs. k_0^2 graph from linearity happens at much lower frequencies. Indeed for the 70% glycerin, the highest frequency for which reliable data was obtained is only 167 Hz. Nevertheless, the effect of viscosity on the slope of the graph is clearly evident.

When the viscosity and density of the mixtures are known, the dispersion data provides excellent experimental values of the surface tension. Viewed in this light our system provides a non-contact method of measuring the surface tension of viscous liquids. Fig. 10 gives the surface tension of the glycerin-water binary mixtures as a function of concentration.

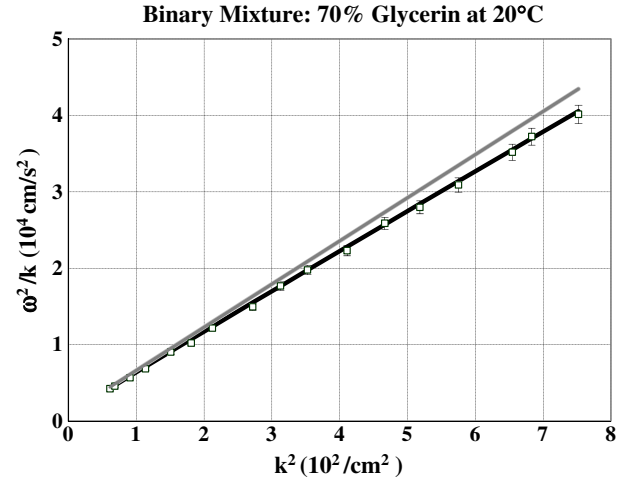

Fig. 9. Dispersion data for capillary waves plotted as ω^2/k_0 vs. k_0^2 for the binary mixture with 70% glycerin at 20 °C. The solid line is a fit using Eq. (10) in the text. The gray line is a fit using Eq. (11), which does not take the effect of viscosity into account.

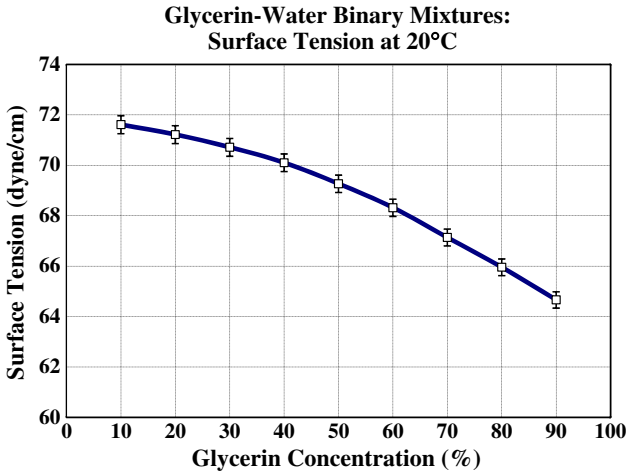

Fig. 10. Surface tension of the glycerin–water binary mixtures as a function of glycerin concentration at 20 °C. The values are obtained from the slope of the graphs of ω^2/k_0 vs. k_0^2 for the concentrations shown. Pure glycerin has a surface tension of 63.4 dyne/cm and a density of 1.26 g/cm^3.

Finally we note that surface tension measurements obtained from surface light scattering on thermal capillary waves tend to underestimate the surface tension because the dispersion of short wavelength capillary waves is greatly affected even when the viscosity is small. This is because the $(8\eta^3\omega/\rho^3)^{1/2}$ term in Eq. (10) grows with frequency and becomes substantial relative to the σ/ρ term. Indeed we may rewrite Eq. (10) as

$$\omega^2 / k_0 = g + (\sigma_{eff} / \rho)k_0^2 \tag{12}$$

where σ_{eff} is the effective surface tension. Since the frequency dependent term comes with a minus sign, dispersion data on thermal capillary waves will tend to give a low value for the effective surface tension. Recently, Fradin, et al. have reported as much as 75% reduction in surface energy of liquid interfaces at submicron length scales [13].

References

[1] H. Lamb, Hydrodynamics, 6th Ed, Dover, New York, 1945, p. 627.
[2] E.H. Lucassen-Reynders, J. Lucassen, Properties of capillary waves, Adv. Coll. And Interface Sci. 2 (1969) 347–395.
[3] J.C. Earnshaw, C.J. Hughes, High frequency capillary waves on the clean surface of water, Langmuir 7 (1991) 2419–2421.
[4] R.H. Katyl, U. Ingard, Line broadening of light scattered from liquid surface, Phys. Rev. Lett. 19 (1967) 64–67.
[5] D. Langevin, Light Scattering by Liquid Surfaces and Complementary Techniques, Dekker, New York, 1992.
[6] J.C. Earnshaw, Surface light scattering: a methodological review, Appl. Opt. 36 (1997) 7583–7592.
[7] D.M. Buzza, General theory for capillary waves and surface light scattering, Langmuir 18 (2002) 8418–8435.
[8] J.S. Huang, W.W. Webb, "Viscous damping of thermal excitations on the interface of critical fluid mixtures", Phys. Rev. Lett. 23 (1969) 160–163.
[9] C. Martel, E. Knobloch, Damping of nearly inviscid water waves, Phys. Rev. E 56 (1997) 5544–5548.
[10] P. Tin, J.A. Mann, W.V. Meyer, T.W. Taylor, Fiber-optics surface light scattering spectrometer, Appl. Opt. 36 (1997) 7601.
[11] D. Richard, E. Raphael, Capillary–gravity waves: the effect of viscosity on the wave resistance, Europhys. Lett. 48 (1999) 49–52.
[12] P. Cicuta, I. Hopkinson, "Dynamic light scattering from colloidal fractal monolayers", Phys. Rev. E 65 (041404) (2002) 1–5.
[13] C. Fradin, A. Braslau, et al., Reduction in surface energy of liquid interfaces at short length scales, Nature 403 (2000) 871–874.
[14] A. Madsen, T. Seydel, M. Sprung, C. Gutt, M. Tolan, G. Grubel, Capillary waves at the transition from propagating to overdamped behavior, Phys. Rev. Lett. 92 (2004) 6104–6107.
[15] P. Cicuta, I. Hopkinson, Recent development of surface light scattering as a tool for optical-rheology of polymer monolayers, Colloids Surf. A Physicochem. Eng. Aspects 233 (2004) 97–107.
[16] K.Y. Lee, T. Chou, D.S. Chung, E. Mazur, Capillary wave damping in heterogeneous monolayers, J. Phys. Chem. 97 (1993) 12876–12878.
[17] U-Ser Jeng, Levon Esibov, Lowell Crow, Albert Steyerl, "Viscosity effect on capillary waves at liquid interfaces", J. Phys. Condens. Matter 10 (1998) 4955–4962.
[18] C.H. Sohl, K. Miyano, J.B. Ketterson, Novel technique for dynamic surface tension and viscosity measurements at liquid–gas interfaces, Rev. Sci. Instrum. 49 (1978) 1464–1469.
[19] C.H. Sohl, K. Miyano, J.B. Ketterson, G. Wong, Viscosity and surface-tension measurements on cyanobenzylidene octyloxyaniline using propagating capillary waves: critical behavior, Phys. Rev. A 22 (1980) 1256–1265.
[20] T.M. Bohanon, J.M. Mikrut, B.M. Abraham, J.B. Ketterson, P. Dutta, Fiber-optic detection system for capillary waves: an apparatus for studying liquid surfaces and spread monolayers, Rev. Sci. Instrum. 62 (1991) 2959–2962.
[21] F. Behroozi, B. Lambert, B. Buhrow, Direct measurement of the attenuation of capillary waves by laser interferometry: non-contact determination of viscosity, App. Phys. Lett. 78 (2001) 2399–2402.
[22] F. Behroozi, J. Smith, W. Even, Stokes' Dream: Measurement of Fluid Viscosity from the Attenuation of Capillary Waves, Am. J. Phys. 78 (2010) 1165–1169.
[23] F. Behroozi, United States Patent # 6,563,588 B2: "Apparatus and Method for Measurement of Fluid Viscosity", issued on May 13, 2003.
[24] F. Behroozi, P.S. Behroozi, Efficient deconvolution of noisy periodic interference signals, J. Opt. Soc. Am. A 23 (2006) 902–905.